



The Two-Component System RstA/RstB Regulates Expression of Multiple Efflux Pumps and Influences Anaerobic Nitrate Respiration in *Pseudomonas fluorescens*

Di-Yin Li,^b Jian-Ting Han,^a Meng-Yuan Zhang,^a Xu Yan,^a  Nannan Zhang,^c Honghua Ge,^c Zhiping Wang,^b Yong-Xing He^a

^aMinistry of Education Key Laboratory of Cell Activities and Stress Adaptations, School of Life Sciences, Lanzhou University, Lanzhou, P.R. China

^bInstitute of Urology, Lanzhou University Second Hospital, Key Laboratory of Urological Diseases in Gansu Province, Gansu Nephro-Urological Clinical Center, Lanzhou, P.R. China

^cSchool of Life Sciences, Anhui University, Hefei, P.R. China

ABSTRACT Multidrug resistance (MDR) efflux pumps are involved in bacterial intrinsic resistance to multiple antimicrobials. Expression of MDR efflux pumps can be either constitutive or transiently induced by various environmental signals, which are typically perceived by bacterial two-component systems (TCSs) and relayed to the bacterial nucleoid, where gene expression is modulated for niche adaptation. Here, we demonstrate that RstA/RstB, a TCS previously shown to control acid-induced and biofilm-related genes in *Escherichia coli*, confers resistance to multiple antibiotics in *Pseudomonas fluorescens* by directly regulating the MDR efflux pumps EmhABC and MexCD-OprJ. Moreover, we show that phosphorylation of the conserved Asp52 residue in RstA greatly enhances RstA-DNA interaction, and regulation of the multidrug resistance by RstA/RstB is dependent on the phosphorylation of the RstA Asp52 residue by RstB. Proteome analysis reveals RstA/RstB also positively regulates the efflux pump MexEF-OprN and enzymes involved in anaerobic nitrate respiration and pyoverdine biosynthesis. Our results suggest that, by coupling the expression of multiple efflux pumps and anaerobic nitrate respiration, RstA/RstB could play a role in defense against nitrosative stress caused by anaerobic nitrate respiration.

IMPORTANCE Microenvironmental hypoxia typically increases bacterial multidrug resistance by elevating expression of multidrug efflux pumps, but the precise mechanism is currently not well understood. Here, we showed that the two-component system RstA/RstB not only positively regulated expression of several efflux pumps involved in multidrug resistance, but also promoted expression of enzymes involved in anaerobic nitrate respiration and pyoverdine biosynthesis. These results suggested that, by upregulating expression of efflux pumps and pyoverdine biosynthesis-related enzymes, RstA/RstB could play a role in promoting bacterial tolerance to hypoxia by providing protection against nitrosative stress.

KEYWORDS two-component system, efflux pumps, multidrug resistance, *Pseudomonas fluorescens*

Rapidly sensing and responding to environmental stimuli is essential for bacteria to survive in constantly changing environments. Two-component systems (TCSs), which are ubiquitously distributed in prokaryotic genomes, play a pivotal role in bacterial sensing and responding to changes in their environment (1). A TCS comprises a sensor kinase and a response regulator, which are usually encoded adjacently in genomes (2, 3). A typical sensor kinase is composed of an N-terminal sensor domain facing the extracellular or periplasmic space and a C-terminal histidine kinase domain located in the cytosol (4). These two domains are connected by a transmembrane

Citation Li D-Y, Han J-T, Zhang M-Y, Yan X, Zhang N, Ge H, Wang Z, He Y-X. 2021. The two-component system RstA/RstB regulates expression of multiple efflux pumps and influences anaerobic nitrate respiration in *Pseudomonas fluorescens*. mSystems 6:e00911-21. <https://doi.org/10.1128/mSystems.00911-21>.

Editor Zackery Bulman, University of Illinois at Chicago

Copyright © 2021 Li et al. This is an open-access article distributed under the terms of the [Creative Commons Attribution 4.0 International license](https://creativecommons.org/licenses/by/4.0/).

Address correspondence to Zhiping Wang, erywzp@lzu.edu.cn, or Yong-Xing He, heyx@lzu.edu.cn.

Received 16 July 2021

Accepted 7 October 2021

Published 2 November 2021

region which differs considerably in various TCSs (4). When exposed to environmental stimuli, the sensor domain undergoes drastic conformational changes, which are transmitted to the cytosolic histidine kinase domain through the transmembrane region, leading to auto-phosphorylation of a conserved C-terminal histidine residue in *trans* (5, 6). The phosphoryl group of the histidine residue is then transferred to a conserved aspartate residue of the responsive regulator, leading to its activation and transcription of downstream genes involved in diverse physiological processes such as chemotactic behavior, osmotic regulation, and virulence (7).

The prevalence of antibiotic-resistance in human pathogens has posed a great challenge to the treatment of bacterial infections (8, 9). Bacteria not only can be intrinsically resistant to certain antibiotics, but also acquire antibiotic resistance via mutations or horizontal gene transfers of antibiotic resistance genes (10). Three major mechanisms are responsible for antibiotic resistance: modification of drug targets, inactivation of antibiotics, and minimization of the intracellular drug concentrations (11). By extruding intracellular antibiotics as well as a wide range of other toxic compounds including heavy metals, solvents, and detergents, the transmembrane efflux pumps play an important role in antibiotic resistance (8, 12). Since aberrant expression of efflux pumps is generally associated with a fitness cost (13), their expressions must be tightly regulated in certain bacterial species, in which efflux pumps were found to be integrated in the complex regulatory networks of TCSs. For instance, Kunihiko et al. reported that over-expression of the responsive regulator component EvgA of the TCS EvgA/EvgS activates the EmrKY efflux pump and accounts for deoxycholate resistance in *Escherichia coli* (14). In *Salmonella*, the TCS BaeS/BaeR was demonstrated to regulate MdtABC and AcrD efflux pumps, which are related with the resistance to novobiocin and β -lactams antibiotics (15). Most recently, a number of other TCSs including AdeS/AdeR (16), CzcR/CzcS (17), AmgR/AmgS (18), and ParS/ParR (19) were found to be involved in regulating efflux pumps of antibiotics, highlighting the important role of TCSs in antibiotic resistance.

Pseudomonas fluorescens is a widely distributed environmental microbe which produces a variety of antibiotics through secondary metabolism to antagonize other competing bacteria and fungi. It also includes virulent strains involved in opportunistic infections (20–23). As *P. fluorescens* can be resistant to a wide spectrum of antibiotics (24), it is therefore urgent to better understand the multidrug-resistance mechanism of *P. fluorescens*. In *P. fluorescens* 2P24, the RND (resistance-nodulation-cell division) superfamily efflux pump EmhABC is characterized to be a key determinant to the resistance toward multiple antibiotics including ampicillin, chloramphenicol, and tetracycline (25, 26). However, it is still elusive if there are any other efflux pumps responsible for the multidrug resistance and how these efflux pumps are regulated in *P. fluorescens*. In this work, we demonstrate that RstA/RstB, a TCS previously shown to control acid-induced and biofilm-related genes in *E. coli* (27), confers resistance to multiple antibiotics in *P. fluorescens* by directly regulating the MDR efflux pumps EmhABC and MexCD-OprJ. Phosphorylation of the conserved Asp52 residue of RstA by RstB was shown to be essential for the regulation function of RstA/RstB. Based on proteome analysis, we identify that RstA/RstB also positively regulated the efflux pump MexEF-OprN and enzymes involved in anaerobic nitrate respiration and pyoverdine biosynthesis, and propose a role for RstA/RstB in the cellular defense against nitrosative stress.

RESULTS

Cofitness analysis in *P. fluorescens* revealed a RstA/RstB-like TCS potentially involved in antibiotic resistance. The similarity of fitness under different growth conditions between any two different deletion strains has been defined as the cofitness (28), and two genes that have a high cofitness value tend to share similar biological functions. High-throughput data sets of microbial fitness had been proved to be informative in predicting gene functions and recently genome-wide mutant fitness data from 32 diverse bacteria across a set of growth conditions were available from <http://fit.genomics.lbl.gov/>, prompting us to seek the possible genes related to antibiotic resistance. In *P. fluorescens*,

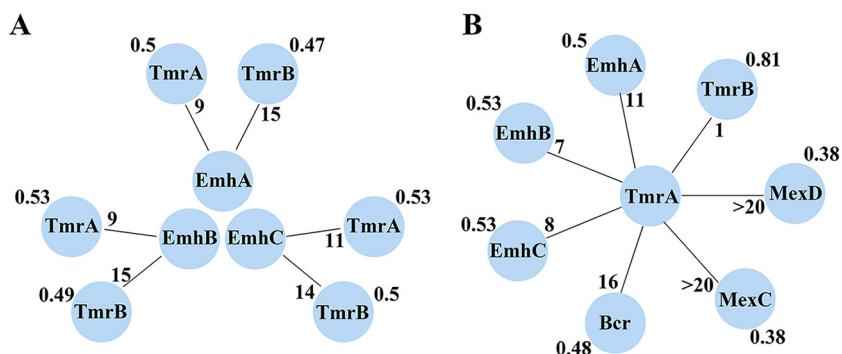


FIG 1 Cofitness values and ranks of (A) RstA/RstB and EmhABC, (B) RstA and other seven genes. The rank of each correlation is marked in the inner circle and cofitness values are marked on the outer ring.

the protein products encoded by the *emhABC* operon were characterized to constitute an efflux pump playing a critical role in antibiotic resistance (25), we therefore reasoned that the strain lacking the resistance related genes should have high cofitness values with strains lacking the EmhABC efflux pump. Using the cofitness browser database, we analyzed the cofitness data of the mutant strains of *P. fluorescens* FW300-N2E2 with deletion of the genes *Pf6N2E2_2823*, *Pf6N2E2_2824*, and *Pf6N2E2_2825*, which are orthologues of *emhA*, *emhB* and *emhC*, respectively (~98% sequence identity). Interestingly, two mutant strains with deletion of either *Pf6N2E2_463* or *Pf6N2E2_464* showed high cofitness values with above-mentioned three mutant strains (Fig. 1A), suggesting these two genes are likely to be related to antibiotic resistance. The genes *Pf6N2E2_463* and *Pf6N2E2_464*, respectively, encode a responsive regulator and sensor kinase of a TCS, which shares moderate sequence identities with the well-characterized RstA/RstB TCS (sequence identity 43%/35%) from *E. coli*. We next analyzed the cofitness data of $\Delta Pf6N2E2_463$ and found that three more mutant strains devoid of genes encoding other efflux pumps (*Pf6N2E2_1660*, *Pf6N2E2_1661*, *Pf6N2E2_3484*) have high cofitness values with the $\Delta Pf6N2E2_463$ strain (Fig. 1B). The genes *Pf6N2E2_1660* and *Pf6N2E2_1661* are orthologues of the components of the MexCD efflux pump from *Pseudomonas aeruginosa* while *Pf6N2E2_3484* encodes a putative dipeptide transporter sharing 39% sequence identity with the bicyclomycin resistance protein Bcr in *E. coli*. Taken together, the cofitness analysis suggests that the RstA/RstB-like TCS (*Pf6N2E2_463* and *Pf6N2E2_464*) are likely to be involved in antibiotic resistance by regulating multiple efflux pumps including the EmhABC (*Pf6N2E2_2823*, *Pf6N2E2_2824*, and *Pf6N2E2_2825*), MexCD (*Pf6N2E2_1660*, *Pf6N2E2_1661*), and Bcr-like (*Pf6N2E2_3484*) pumps in *P. fluorescens*.

The TCS RstA/RstB and MexCD-OprJ efflux pump contribute to antibiotic resistance in *P. fluorescens* 2P24. To validate the potential antibiotic resistance related genes identified by cofitness analysis, we found the corresponding orthologues of these genes in the genome of *P. fluorescens* 2P24 (Table S3), constructed the single deletion mutants and measured the MICs of these mutants. *PFLP_02434* and *PFLP_02435* in *P. fluorescens* 2P24 correspond to *Pf6N2E2_463* and *Pf6N2E2_464*, respectively, and were named *rstA/rstB* as they encode proteins with the highest BLASTP score (43.85%/34.69% identity) with *E. coli* RstA/RstB proteins among the ORFs of *P. fluorescens* 2P24. Deletion of either of these two genes leads to increased susceptibility to multiple antibiotics including ampicillin, gentamicin, chloramphenicol, kanamycin, lomefloxacin, and tetracycline (Table 1). The *mexC* (*PFLP_03468*) deletion mutant, along with the *emhABC* deletion mutant, also showed decreased resistance to multiple drugs, yet with a slightly different antibiotic spectrum, suggesting different substrate specificities for these two efflux systems. The mutant devoid of the MFS transporter *PFLP_00760*, a homologous protein of Bcr, did not show significantly altered susceptibility to all the tested antibiotics (Table 1). Collectively, we identified the TCS RstA/RstB

TABLE 1 Susceptibilities of the wild-type strain of *P. fluorescens* 2P24 and its constructed mutants to various antimicrobial agents

Strain	MIC ($\mu\text{g/mL}$) ^a					
	Amp	Chl	Kan	Tet	Gen	Lmf
Wild-type	512	128	4	8	2	0.5
ΔrstA	256	32	1	4	<0.25	<0.25
ΔemhABC	8	32	1	1	0.5	<0.125
ΔmexC	512	32	0.5	4	1	<0.25
Δbcr	512	64	4	16	4	1
$\Delta\text{rstB-SD}$	256	128	2	4	1	0.5
$\Delta\text{rstB-KD}$	256	32	2	4	0.5	<0.25
$\text{rstA}^{\text{D52A}}$	512	16	2	4	0.5	<0.25
$\text{rstA}^{\text{D52E}}$	256	16	0.5	2	<0.25	<0.25

^aAmp, ampicillin; Chl, chloramphenicol; Kan, kanamycin; Tet, tetracycline; Lmf, lomefloxacin.

and the MexCD-OprJ efflux pump are involved in antibiotic resistance of *P. fluorescens* 2P24.

RstA positively regulates the expression of *emhABC* and *mexCD-OprJ*. Given that the TCS RstA/RstB was shown to be related to antibiotic resistance, we asked whether the RstA regulator controls the expression of the multidrug efflux pumps EmhABC and MexCD-OprJ. Using the *lacZ* reporter fusion of the *emhA* promoter, we showed that expression of the *emhABC* operon was significantly decreased in the *rstA* deletion strain (ΔrstA) compared with that of the wild-type strain (Fig. 2A). Consistently, qRT-PCR assay revealed that deletion of *rstA* led to more than a 3-fold decrease of the *emhA* and *emhC* transcription levels (Fig. 2B). Moreover, by using qRT-PCR, we found that the ΔrstA strain showed a 10-fold decrease in *mexC* transcription level compared with the wildtype strain (Fig. 2B). Taken together, our results demonstrated that the responsive regulator RstA activates the expression of efflux pumps EmhABC and MexCD-OprJ in *P. fluorescens* strain 2P24.

RstA binds to the promoter of *emhABC* and *mexCD-OprJ* in a phosphorylation dependent manner. Given the regulatory role of RstA on EmhABC and MexCD-OprJ, we asked whether the RstA protein could directly interact with the promoter regions of the *emhABC* and *mexCD-OprJ* operons. The 265-bp upstream sequence of *emhA* was amplified and it was shown by using the electrophoretic mobility shift assays (EMSAs) that this DNA sequence weakly interact with RstA fused with an N-terminal maltose binding protein tag (MBP-RstA). As the DNA-binding ability of responsive regulators is generally dependent on phosphorylation of a conserved Asp residue, we performed an *in vitro* phosphorylation assay in which the MBP-RstA protein was incubated with acetyl phosphate, a high-energy phosphoryl-donor known to phosphorylate the conserved Asp residues in responsive regulators (29). Notably, the phosphorylated MBP-RstA (MBP-RstA^P) interacted with the upstream sequence of *emhA* in a concentration dependent manner as shown by the EMSA (Fig. 3A). Moreover, phosphorylation of the MBP-RstA protein by acetyl phosphate also significantly enhanced its binding affinity toward the 101-bp upstream region of *mexCD-OprJ* (Fig. 3B). The appearance of two shifted bands for the *mexC* promoter suggested the presence of two RstA-binding sites, one with high binding affinity and another with low binding affinity. We also showed that MBP did not interact with the DNA probes used in the EMSAs (Fig. S1), excluding the possibility that MBP could interfere with the DNA-binding assays of RstA.

Although we attempted to use LC-MS/MS to pinpoint the phosphorylation sites of the MBP-RstA protein upon treatment by acetyl phosphate, however, no phosphorylated Asp residues were detected (data not shown). This is most likely due to the labile nature of phosphorylated Asp, which has an extremely short half-life and was notoriously difficult to capture. We next performed a multiple sequence alignment and identified that the Asp52 residue of RstA was strictly conserved among responsive regulators from various bacterial species (Fig. S2). The corresponding Asp residues in responsive regulators, such as CusR from *E. coli* (30), AlgR (31) and CpxR (32) from *P. aeruginosa*, have been reported to receive the phosphor-group from their cognate sensor kinases. To confirm if the 52 Asp residue of

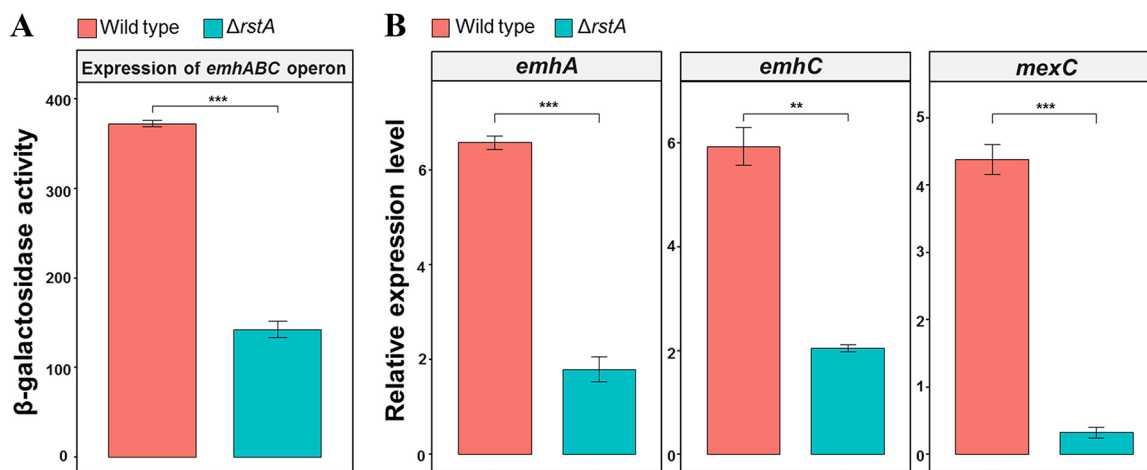


FIG 2 RstA positively regulates the expression of efflux pump *emhABC* and *mexCD*. (A) The β -galactosidase activities of wild-type strain and $\Delta rstA$. (B) The transcription levels of *emhA*, *emhC* and *mexC* were measured in wild-type and $\Delta rstA$ strain via qRT-PCR assays. The expression level of 16S was used for normalization and $2^{-\Delta Ct}$ method was used for data analysis. Error bars denote standard deviation ($n = 3$). P less than 0.01 was displayed as **, P less than .05 was displayed as *.

RstA is essential for the DNA-binding capacity, we purified the MBP-fused D52A mutant protein of RstA (MBP-RstA^{D52A}) and tested its DNA-binding capacity. It was revealed that, compared with its wild-type counterpart, MBP-RstA^{D52A} had significantly compromised DNA-binding affinities toward the upstream sequences of *emhABC* and *mexCD-oprJ* regardless of the acetyl phosphate treatment (Fig. 3C and D). These results suggest the 52 Asp residue of RstA is likely to be the phosphorylation site that modulate the RstA-DNA interactions.

Phosphorylation of the Asp52 residue of RstA by the RstB kinase contributes to the antibiotic resistance of *P. fluorescens* 2P24. To investigate whether phosphorylation of RstA contributes to the antibiotic resistance of *P. fluorescens* 2P24, we constructed the mutant strain bearing the *rstA*^{D52A} single site mutation and tested its antibiotic resistance. Like the $\Delta rstA$ strain, this *rstA*^{D52A} mutant strain showed increased susceptibility to several antibiotics including chloramphenicol (8 folds), gentamicin (4 folds), kanamycin (2 folds), and lomefloxacin (>2 folds) (Table 1). Moreover, deletion of the *rstB*-kinase domain ($\Delta rstB$ -KD) also led to increased antibiotic susceptibility. Consistently, the expression levels of *emhA*, *emhC*, and *mexC* were significantly

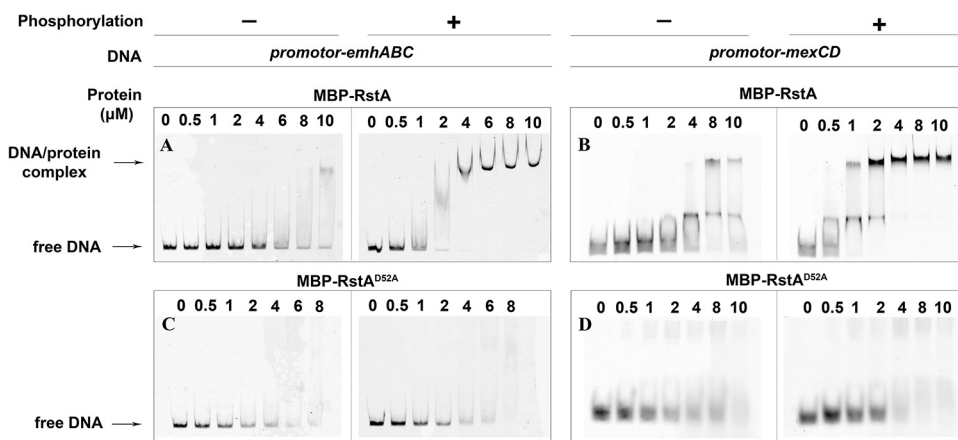


FIG 3 The EMSAs were used to determine the interaction between promoter-*emhABC* and RstA, phosphorylated-RstA (A, B), RstA^{D52A} or phosphorylated-RstA^{D52A} (C, D). The binding between promoter-*mexC* and RstA, phosphorylated-RstA, RstA^{D52A}, or phosphorylated-RstA^{D52A} was determined with the same methodology. The concentrations of protein were labeled at the top of each lane. The protein phosphorylation state was indicated with + or -, respectively.

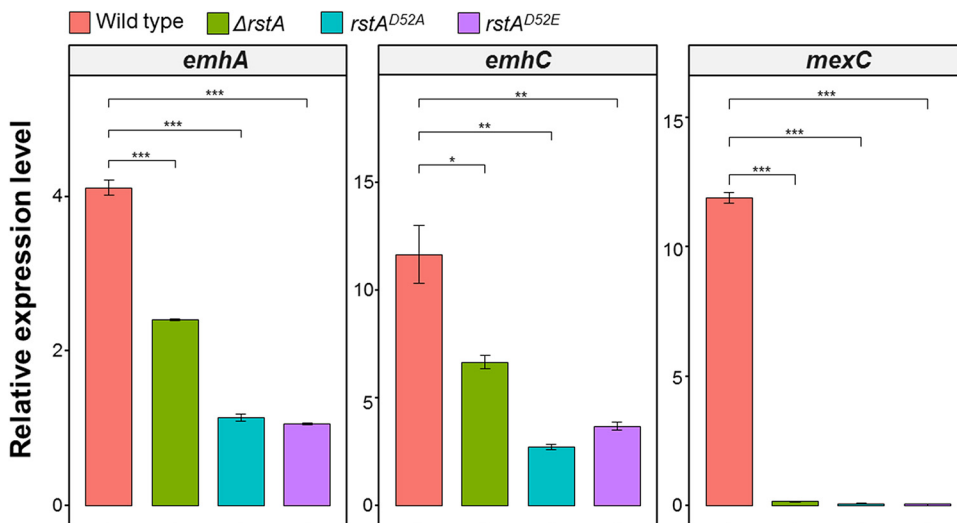


FIG 4 The qRT-PCR assays were employed to monitor the transcription levels of *emhA*, *emhC*, and *mexC* in different strains. The expression level of 16S was used for normalization and $2^{-\Delta\Delta Ct}$ method was used for data analysis. Error bars denote standard deviation ($n = 3$). P less than 0.001 was displayed as ***, P less than 0.01 was displayed as **, P less than 0.05 was displayed as *.

decreased in the $rstA^{D52A}$, $rstA^{D52E}$, and $\Delta rstA$ mutant strains compared with the wild-type strain (Fig. 4). It is interesting to note that *emhAC* expression is even less in the $rstA^{D52A}$ strain than in the $rstA$ deletion strain, suggesting that *rstA* may regulate some unknown factors that influence *emhAC* expression in a phosphorylation independent manner.

Interestingly, deletion of the sensor domain of *rstB* ($\Delta rstB$ -SD) had little effect on the antibiotic resistance (Table 1), implying either the intracellular kinase domain of RstB could be activated through cross-regulation by other TCSs or the ligands recognized by the sensor domain of RstB were absent in the culture medium. Taken together, our data indicates that phosphorylation of the Asp52 site of RstA by the sensor kinase RstB plays an important role in regulating antibiotic resistance.

The responsive regulator RstA influences multiple physiological processes including nitrate respiration, pyoverdine biosynthesis, and drug efflux. In order to characterize the potential regulons of RstA in *P. fluorescens* 2P24, we performed label-free quantitative proteomics profiling of the wild-type and $\Delta rstA$ mutant strains. In total 2,354 proteins were identified with 1% false discovery rate (FDR), and hierarchical clustering using z-scored intensities of the 275 proteins quantified with high confidence (P value < 0.05) showed that four replicates of the samples of *P. fluorescens* and its derivatives $\Delta rstA$ were correctly clustered together (Fig. S3). Student's *t* test was used to screen differential expression proteins (DEPs) with fold change greater than 1.5 and P value less than 0.05 was used as thresholds, resulting in 33 upregulated proteins and 153 downregulated proteins (Fig. 5A). Gene ontology (GO) enrichment analysis revealed these DEPs were involved in many biological processes, especially antibiotic biosynthetic process, arginine metabolic process, and stress responses (Fig. 5B). To further study the biological pathways modulated by RstA, the interaction networks of downregulated proteins were created using the STRING database, showing that the downregulated proteins mainly participate in biological processes of pyoverdine biosynthesis and iron transport, nitrogen metabolism, bacterial chemotaxis, arginine metabolism, and efflux activities (Fig. 5C). Notably, several proteins including NarG1, NarG2, NarH, NarI, NarJ, NarU, NirE, NirF, NirG, and NirN involved in nitrate or nitrite reductase systems were markedly decreased in the $\Delta rstA$ strain (Fig. 5A). Moreover, proteins involved in pyoverdine biosynthesis including PvdA, PvdD, PvdE, PvdH, PvdL, PvdM, PvdO, PvdJ1, and PvdJ2 (33) were also significantly downregulated in the $\Delta rstA$ strain. The proteomic data also indicated that, in addition to the MexCD efflux pump,

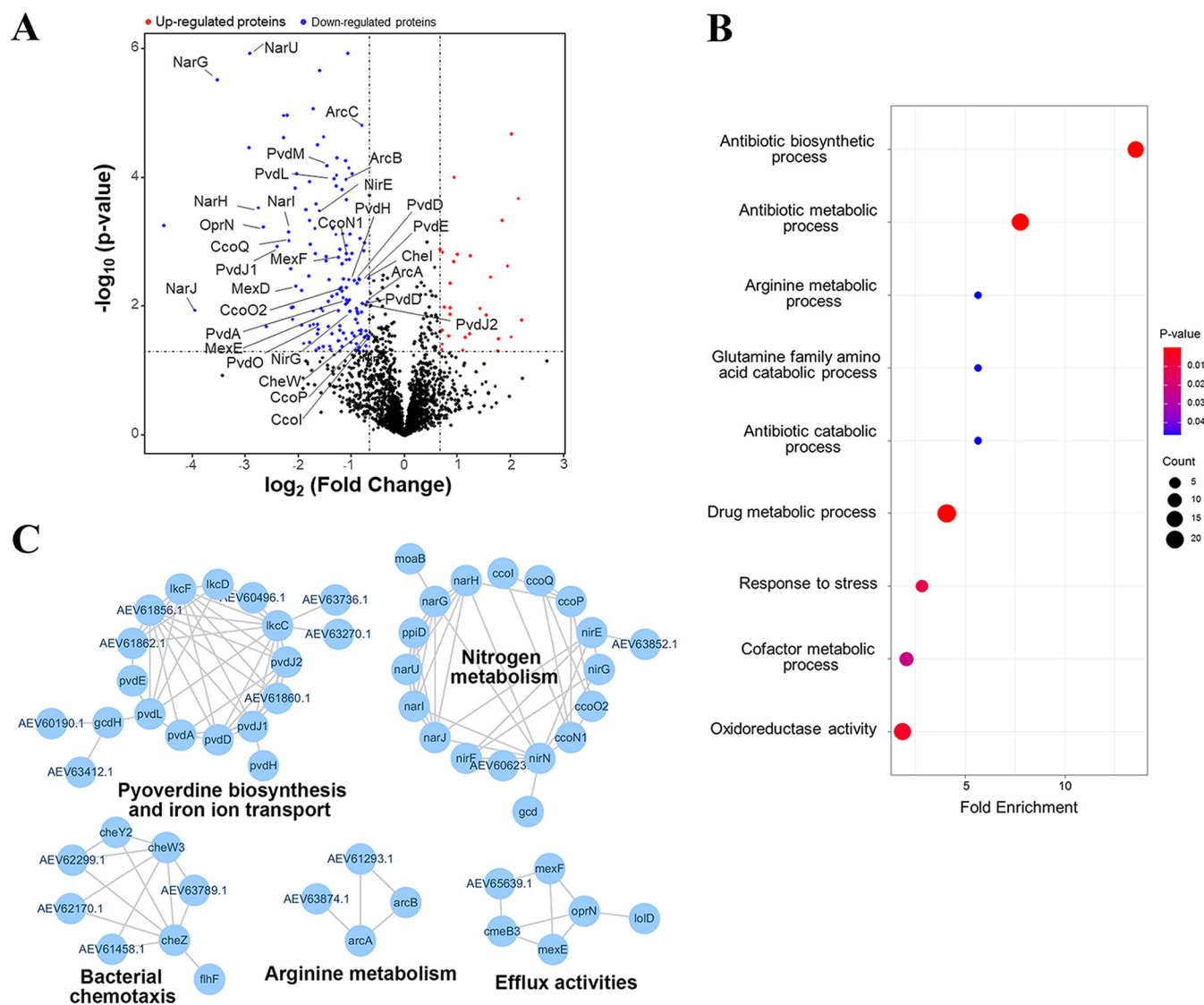


FIG 5 Comparative proteomic analysis of the wild-type and *RstA* mutant strains. (A) A volcano plot showing the differentially expressed genes (DEPs) in the $\Delta RstA$ and $D52A$ strain compared with the wild-type strain of *P. fluorescens* 2P24. The red and blue dots indicate upregulated and downregulated genes, respectively, which are filtered based on the cut-off values of $|\log_2(\text{FoldChange})| > 1.5$ and adjusted *P* value less than 0.05. (B) Fisher's exact test of *RstA*-affect proteins with the thresholds of *P* value less than 0.05 and enrichment factor greater than 1.5. The *P* value and protein count were represented with dot color and circle size. (C) STRING network analysis of DEPs in the $\Delta rstA$ and $rstA^{D52A}$ strain. Each node represents one protein and the interaction between proteins was displayed with lines.

MexEF-OprN, an efflux pump that can extrude a variety of antibiotics as well as quorum sensing signals (34), was decreased in the $\Delta rstA$ strain. Collectively, our proteomic analysis demonstrated that the responsive regulator *RstA* not only activates the expression of several efflux pumps, but influences nitrate respiration and pyoverdine biosynthesis as well.

DISCUSSION

Multidrug efflux pumps play an essential role in bacterial antibiotic resistance in both clinical and environmental settings (35, 36). The RND superfamily of efflux pumps, which are specific to Gram-negative bacteria and always form a tripartite complex spanning across the inner and outer membranes, are implicated in multidrug resistance in many bacterial species including the prominent human pathogens *P. aeruginosa*, *E. coli*, and *Salmonella* (37). In *P. aeruginosa*, there are several encoded RND-type efflux systems, four of which, i.e., MexAB-OprM, MexCD-OprJ, MexEF-OprN, and

MexXY-OprM are characterized to be the significant determinants of multidrug resistance. Complex regulatory networks including multiple transcription regulators (MexR, MexT, NalC, NalD, NfxB, etc.) are involved in tight control of the expression levels of these efflux pumps. Disruption of the regulatory network that leads to upregulation of the efflux pumps have been commonly found in clinical isolates exhibiting the MDR phenotype. Being a close relative of *P. aeruginosa*, *P. fluorescens* produces a variety of antimicrobials and at the same time intrinsically resistant to multiple antibiotics, yet questions remain how the antibiotic resistance in *P. fluorescens* is regulated. Our work demonstrated that the TCS RstA/RstB contributes to antibiotic resistance of *P. fluorescens* by activating expression of the EmhABC and MexCD-OprJ efflux pumps, highlighting the important roles of certain TCSs in modulating intrinsic antibiotic resistance. In *E. coli* and *Salmonella*, RstA was reported to regulate genes related to biofilm formation and iron acquisition (27, 38), and the classic RstA binding motif (TACAN₆TACA) was not found in the promoter regions of major antibiotic efflux pumps in these bacterial species (39). These results suggest an evolutionarily divergent role of RstA/RstB in regulating RND efflux pump expression among different bacterial species.

As bacteria are constantly exposed to different levels of antibiotics or toxic compounds, it is unsurprising that expression of efflux pumps could be integrated into the TCS regulatory network, which could transiently upregulate the efflux pumps in response to certain effectors or environmental stimuli. When a sensor kinase detects a specific signal, it usually undergoes auto-phosphorylation and subsequently transfer the phosphate group to its cognate responsive regulator, enabling genome-scale transcriptional activation by the responsive regulator (4). Consistently, we found that deletion of the cytosolic kinase domain of RstB leads to antibiotics susceptibility, confirming the essential role of the RstB kinase domain in activating the RstA responsive regulator. Sequence analysis indicates that RstA belongs to the OmpR/PhoB protein family, which comprises approximately 40% of all response regulators. Notably, the conserved D52 residue was pinpointed as the phosphorylation site modulating the DNA binding affinity of RstA and mutation of this aspartate into Ala leads to the decreased antibiotic resistance of *P. fluorescens*, highlighting that phosphorylation of D52 acts as a molecular switch governing the activity of RstA. It was previously shown that for the OmpR/PhoB family responsive regulators such as DrrB, DrrD (40), and MtrA (41), phosphorylation of the conserved aspartate residue promotes dimerization and brings the DNA-binding domains into proximity, resulting in the enhanced DNA-binding affinity. Collectively, our data support that a conserved phosphorylation-dependent regulation mechanism is shared among the responsive regulators of the OmpR/PhoB family.

What kind of signals the sensor domain of RstB detects is currently unknown. Interestingly, deletion of the RstB sensor domain barely affects the antibiotic resistance of *P. fluorescens*, suggesting that the histidine kinase domain of RstB could either be phosphorylated by other sensor kinases or undergo basal auto-phosphorylation without any extracellular signal input. By using the three-dimensional structure prediction server Phyre we found that the RstB extracellular domain is predicted to share a similar structural fold with the NarQ extracellular domain (42), despite the low sequence identity (~23%). NarQ, together with NarX, are known to be sensor kinases that respond to nitrate and nitrite to regulate enzymes involved in anaerobic respiration and fermentation (43, 44). Moreover, our proteomic data clearly demonstrated that the responsive regulator RstA positively regulates the enzymes involved in anaerobic nitrate respiratory chain (NarG, NarH, NarI, NarJ, NarK) (45, 46) and arginine deiminase pathway (ArcA, ArcB, ArcC, ArcD) (47), which are typical regulons of NarQ. All these pieces of evidence direct to a possible role in sensing nitrate/nitrite/their analogues and regulating anaerobic nitrate respiration and arginine fermentation for the TCS RstA/RstB.

Several *Pseudomonas* species including *P. fluorescens* can perform denitrification under anaerobic conditions, using nitrate instead of oxygen as a terminal electron acceptor (48). This process, also known as anaerobic nitrate respiration, generally results in the formation of NO and/or other reactive nitrogen species which exert

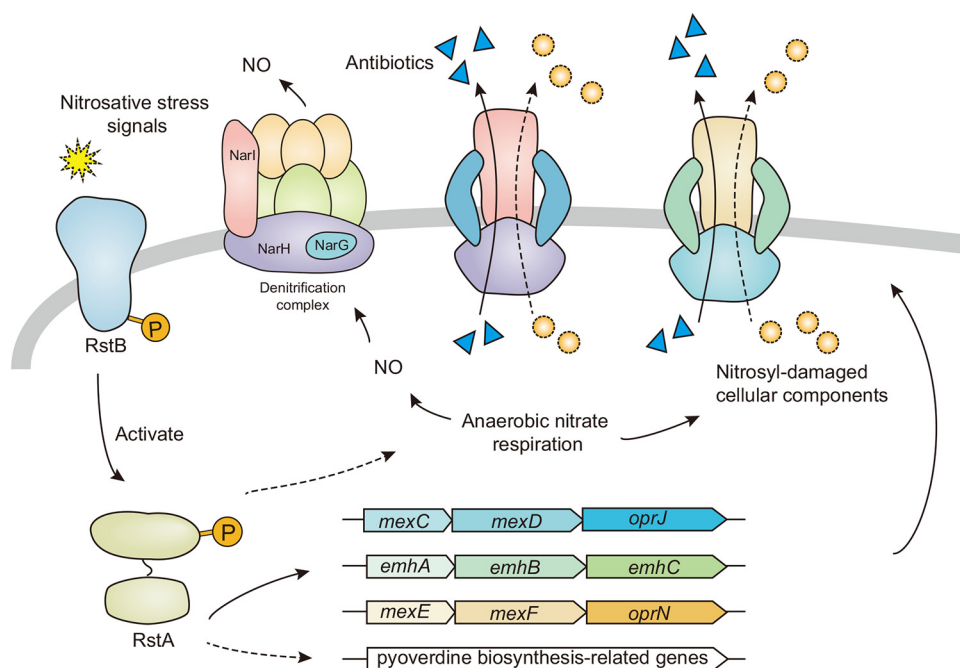


FIG 6 A working model for the physiological roles of RstA/RstB under nitrosative stress of *P. fluorescens* 2P24. During anaerobic nitrate respiration in *P. fluorescens* 2P24, RstB is activated by sensing relative signal molecules and activates RstA which upregulates expression of efflux pumps and pyoverdine biosynthesis-related enzymes. This process not only protects cells against nitrosative damage by extruding the nitrosyl-damaged cellular components but increases antibiotic resistance. The solid arrows denote direct regulations while the dashed arrows denote indirect regulations.

nitrosative stress on the cells (49). Therefore, the sensing of such compounds as well as the induction of nitrosative stress defense against proteins appears to be vital for cell proliferation. The multidrug efflux pump MdtEF-TolC in *E. coli* (50) and MexEF-OprN in *P. aeruginosa* (51) had been shown to be induced in response to nitrosative stress and protect against nitrosative damage by extruding the nitrosyl-damaged cellular components. Genes involved in the production of pyoverdine were also implied in resistance to nitrosative stress (52). It is therefore likely that RstA/RstB can function as a sensor for nitrosative stress, and upregulates expression of efflux pumps and pyoverdine biosynthesis-related enzymes to protect against nitrosative stress (Fig. 6). On the other hand, overexpression of efflux pumps leads to enhanced consumption of oxygen, causing microenvironmental hypoxia, which in turn promotes anaerobic nitrate respiratory in *P. aeruginosa* (13). It should be interesting to investigate how the TCS RstA/RstB could be involved in mediating the interplay between expression of efflux pumps, biosynthesis of pyoverdine and anaerobic nitrate respiration in the future.

MATERIALS AND METHODS

Bioinformatics analysis. The homozygous cofitness data of Pf6N2E2_2823, Pf6N2E2_2824, Pf6N2E2_2825, Pf6N2E2_463, Pf6N2E2_464, Pf6N2E2_1660, Pf6N2E2_1661, and Pf6N2E2_3484 deletion strains were acquired from the online Cofitness Browser Database (<http://fit.genomics.lbl.gov/>). The sequence alignment was performed using the Basic Local Alignment Search Tool of the NCBI website and the Multalin page (<http://multalin.toulouse.inra.fr/multalin/>).

Bacterial strains, plasmids, and culture conditions. The bacterial strains and plasmids are listed in Table S1. *E. coli* strains were grown at 37°C in Luria-Bertani (LB) broth. *P. fluorescens* 2P24 was grown at 28°C in King's B (KB) medium (31). Ampicillin and kanamycin was used at a concentration of 50 µg/ml.

Deletion of gene loci in *P. fluorescens* 2P24. The in-frame deletion mutants were constructed via double-crossover homologous recombination with the suicide plasmid pK18Km as reported previously (26). For each gene, both flank regions (longer than 1Kb) including 100 bp in-frame were PCR-amplified, respectively, and linked together using overlap PCR. The linked fragment, cloned into pK18mobsacB, was transported into *P. fluorescens* 2P24 by conjugating with the *E. coli* strain WM3064 to replace the target gene locus. In brief, after transformed with the suicide plasmid, the WM3064 and the wild-type

P. fluorescens 2P24 strains were mixed in the same dilution rates and plated on a KB agar plate for 6 h to 8 h. Following scraping little bacterial plaque in the double-stress (ampicillin, kanamycin) KB medium, proper dilutions were plated on a double-stress KB agar plate and single crossover strains were validated and cultured in the KB medium for 8 h. Under a 10% sucrose (wt/vol%) stress, mutant strains were confirmed by PCR amplification after the second crossover.

MIC. The MIC values were identified via a serial dilution method using 96-well cell culture plates which contained graded concentrations (0.25–512 $\mu\text{g/ml}$) of each antibiotic. Strains of log phase ($\text{OD}_{600} = 0.8$) were diluted to a final concentration of $10^5/\text{ml}$ with KB broth and inoculated to each well. After incubated at 28°C for 20 h, the MIC readings of the wells were detected by a microplate reader at a wavelength of 600 nm (Absorbance Reader ELx808, BioTek) (53).

Construction of LacZ fusion reporter plasmid and β -galactosidase assays. We used a kanamycin resistance plasmid pRG970Km to construct *lacZ* fusions as previously reported (54). Purified 270 bp DNA fragments of the upstream sequence of *emhABC* and the plasmids were digested by BamHI and CAIP, after which the fragment was cloned ahead of a promoter-less *lacZ* gene. The plasmid transformation was performed via conjugating between a donor strain (*E. coli* WM3064) and a recipient strain (*P. fluorescens* 2P24) as mentioned above. As reported by Miller before (55), the LacZ expression levels were measured by β -galactosidase assays. Bacterial cultures were grown at 28°C in KB medium to the OD_{600} of 0.5 and the o-nitrophenol (Sigma-Aldrich, St. Louis, MO, USA) coloration, evaluated by absorbances of OD_{550} , OD_{420} , and OD_{650} , was recorded to measure the activity of β -galactosidase (DU530 UV/Vis spectrophotometer, Beckman Coulter, CA, USA). All samples were tested in three duplicates and assays were performed at least three times.

Quantitative real-time PCR assay. Overnight cultured bacterial cells were diluted (1:50) in fresh KB medium and grown to the OD_{600} of 0.25, then 4 ml cultures were harvested by centrifugation at 4°C . After total RNA extraction (Iso plus, TaKaRa, Dalian, China) and cDNA preparation (PrimeScript RT reagent kit with gDNA Eraser, TaKaRa, Dalian, China), qRT-PCR were performed using the SYBR Premix Ex Taq (TaKaRa, Dalian, China) and CFX96 real-time PCR detection system (Bio-Rad, Hercules, CA, USA), all according to the manufacturer's instruction. PCRs were set up using equivalent amounts of cDNA derived from the same amount of input RNA. The concentrations of all nucleic acid samples were measured using a NanoDrop 2000 spectrophotometer (Thermo Fisher Scientific, Inc., USA) and the 260/280 ratio of samples is limited between 1.8 and 2.0. At least three biological replicates were performed. As described previously, $2^{-\Delta\text{Ct}}$ method was used to analyze relative expression levels of target genes and the expression level of 16S in each individual sample was measured as the internal control. The equation used in our study is

$$\text{Relative expression level} = 2^{-(C_{t,X} - C_{t,R})} \times 10^4$$

where $C_{t,X}$ is the threshold cycle for target amplification and $C_{t,R}$ is the threshold cycle for reference (16S) amplification.

Protein expression and purification. The RstA gene was amplified and cloned into pMAL-c2X expression vector containing an additional maltose-binding protein (MBP) tag. The RstA bearing D52A mutation expression plasmid was obtained via overlap PCR. All these recombinant plasmids and the untreated pMAL-c2X were transformed to *E. coli* BL21(DE3) cells, which were developed in LB medium at 37°C supplemented with 50 $\mu\text{g/ml}$ ampicillin. The protein expression was induced by 0.2 mM IPTG when OD_{600} reached 0.6 and cultured at 16°C for another 20 h. After harvested by centrifugation at 5,000 g for 10 min, the cells were resuspended in a column binding buffer containing 20 mM Tris-HCl at pH 8.0, 200 mM NaCl, 1 mM EDTA, 1 mM DTT, and lysed by sonication. The debris was removed via centrifugation at 12,000 g for 30 min and subsequently the supernatant was loaded onto an amylose resin affinity column (New England Biolabs, Inc., USA) for purification of the MBP protein or the MBP-tagged proteins, which were eluted by the binding buffer supplemented with 10 mM maltose. The purified proteins, MBP-RstA, MBP-D52A, and MBP, were concentrated and stored at -80°C for further usage.

Protein phosphorylation *in vitro*. The proteins were phosphorylated *in vitro* as a standard reaction reported before (56). In brief, the protein was diluted into the buffer containing 100 mM Tris-HCl (pH 7.4), 10 mM MgCl_2 , 125 mM KCl, and 50 mM acetyl phosphate (lithium potassium acetyl phosphate, sigma) with a final concentration of 100 $\mu\text{g/ml}$ and incubated for a further 1 h at 30°C . Then the buffer was replaced with 20 mM Tris-HCl (pH 7.4) by a centrifugal filter (Amicon Ultra-0.5 Centrifugal Filter Unit with Ultracel-3 membrane, Millipore). As for control groups, the protein was processed with the same method except acetyl phosphate was removed from the dilution buffer.

Electrophoretic mobility shift assay and DNase I footprinting assay. Promoters of *emhA* and *emhC*, designated as FAM-*emhA* and FAM-*mexC*, were amplified and purified for EMSA and DNase I footprinting assays. For EMSAs, 50 ng of purified promoters were incubated with different amounts of proteins for 30 min at room temperature. In a total volume of 20 μl , the reaction mixture contained 50 mM Tris-HCl at pH 7.5, 10 mM MgCl_2 , 10% (vol/vol) glycerol, 0.5 mM EDTA, 50 mM KCl, and 3 μM bovine serum albumin (BSA) to prevent unspecific binding (54). Separated by 6% native PAGE, electrophoretic bands were detected by a UVP BioSpectrum Imaging system (UVP, CA, USA). For DNase I footprinting assays, 3 pmol DNA was incubated with different concentrations of proteins for 30 min at room temperature as well, followed by digestion with DNase I (Promega) for 2.5 min at 30°C . The reactions were quenched by adding the stop-buffer consisting of 0.15% SDS, 200 mM sodium acetate, and 30 mM EDTA, and then further incubated in a water bath at 70°C for 30 min. The digestion production was extracted with isopropanol/chloroform and precipitated with ethanol and the pellets were dissolved in 30 μl Milli-Q water.

Sample preparation and LC-MS/MS analysis. All proteomics samples were prepared using the modified protocol which had been reported by Matthias Mann et al. (57). Briefly, bacterial cells of the wild-type, $\Delta rstA$, and $rstA^{DS2A}$ strains from early stationary phase ($OD_{600} = 0.8$) were collected and resuspended in 6 M Urea, 100 mM DTT, and 100 mM Tris-HCl (pH 7.0), and proteins were digested with trypsin overnight. The total peptide was desalted with C18-column and dissolved into 0.1% formic acid (FA) at a final concentration of 100 ng/ μ l. For MS analysis, 1 μ g peptide of each sample was subjected to nanoflow liquid chromatography-tandem mass spectrometry analysis on an Orbitrap Fusion Lumos mass spectrometer (Thermo Scientific) coupled online to an EASY-nLC 1200 system in the data-dependent mode. Using a 150 mm \times 75 μ m C18 column with 2 μ m particles, peptides were separated on a 90-min nonlinear gradient: 5%–35% buffer B for 60 min, 35%–80% buffer B for 20 min, and 100% buffer B for 10 min (buffer A: 0.1% FA; buffer B: 80% acetonitrile, 0.1% FA) at 300 nL/min constant flow rate. Source voltage and current were set to 2.5 KV and 100 A, respectively. All MS measurements were performed in the positive ion mode and acquired across the mass range of 300–1,800 m/z . Raw mass spectrometry files were analyzed by ProteinDiscovery (version 2.3) (58) and MS/MS spectra was searched against the full protein sequences of *P. fluorescens* 2P24 with the fixed modification of cysteine carbamidomethylation, and variable modification methionine oxidation configured. Other parameters were set up using the default values and the false discovery rate (FDR) was set to 0.01 for both peptide and protein identifications. Further bioinformatics and statistical analyses were performed using the software Perseus (59).

Data availability. The MS raw files and proteome sequences of *P. fluorescens* 2P24 have been deposited to the ProteomeXchange Consortium via the PRIDE partner repository with the data set identifier PXD018793 (60).

SUPPLEMENTAL MATERIAL

Supplemental material is available online only.

FIG S1, TIF file, 1 MB.

FIG S2, TIF file, 0.5 MB.

FIG S3, TIF file, 1.4 MB.

TABLE S1, DOCX file, 0.02 MB.

TABLE S2, DOCX file, 0.02 MB.

TABLE S3, DOCX file, 0.01 MB.

TABLE S4, DOCX file, 0.03 MB.

ACKNOWLEDGMENT

We thank the mass spectrometry facility at School of Life Sciences of Lanzhou University for support in proteomics data acquisition.

This work was supported by the grants from the National Natural Science Foundation of China (Grant Nos. 31971422, 31970103, and 31770535), Key Research and Development Plan Project of Anhui Province (Grant No. 202004a06020035), and the grant from the State Key Laboratory of Veterinary Etiological Biology (Grant No. SKLVEB2020KFKT013).

REFERENCES

1. Tiwari S, Jamal SB, Hassan SS, Carvalho PVSD, Almeida S, Barh D, Ghosh P, Silva A, Castro TLP, Azevedo V. 2017. Two-component signal transduction systems of pathogenic bacteria as targets for antimicrobial therapy: An overview. *Front Microbiol* 8:1878. <https://doi.org/10.3389/fmicb.2017.01878>.
2. Linsky M, Vitkin Y, Segal G. 2020. A novel *Legionella* genomic island encodes a copper-responsive regulatory system and a single lcm/Dot effector protein transcriptionally activated by copper. *mBio* 11:e03232-19. <https://doi.org/10.1128/mBio.03232-19>.
3. Capra EJ, Laub MT. 2012. Evolution of two-component signal transduction systems. *Annu Rev Microbiol* 66:325–347. <https://doi.org/10.1146/annurev-micro-092611-150039>.
4. Stock AM, Robinson A VL, Goudreau PN. 2000. Two-component signal transduction. *Annu Rev Biochem* 69:183–215. <https://doi.org/10.1146/annurev.biochem.69.1.183>.
5. Jacob-Dubuisson F, Mechaly A, Betton JM, Antoine R. 2018. Structural insights into the signalling mechanisms of two-component systems. *Nat Rev Microbiol* 16:585–593. <https://doi.org/10.1038/s41579-018-0055-7>.
6. Mitrophanov AY, Groisman EA. 2008. Signal integration in bacterial two-component regulatory systems. *Genes Dev* 22:2601–2611. <https://doi.org/10.1101/gad.1700308>.
7. Tierney AR, Rather PN. 2019. Roles of two-component regulatory systems in antibiotic resistance. *Future Microbiol* 14:533–552. <https://doi.org/10.2217/fmb-2019-0002>.
8. Langton KP, Henderson PJF, Herbert RB. 2005. Antibiotic resistance: multidrug efflux proteins, a common transport mechanism? *Nat Prod Rep* 22:439–451. <https://doi.org/10.1039/b413734p>.
9. Brown ED, Wright GD. 2016. Antibacterial drug discovery in the resistance era. *Nature* 529:336–343. <https://doi.org/10.1038/nature17042>.
10. MacLean RC, San Millan A. 2019. The evolution of antibiotic resistance. *Science* 365:1082–1083. <https://doi.org/10.1126/science.aax3879>.
11. Blair JMA, Webber MA, Baylay AJ, Ogbolu DO, Piddock LJV. 2015. Molecular mechanisms of antibiotic resistance. *Nat Rev Microbiol* 13:42–51. <https://doi.org/10.1038/nrmicro3380>.
12. Martinez JL, Sánchez MB, Martínez-Solano L, Hernandez A, Garmendia L, Fajardo A, Alvarez-Ortega C. 2009. Functional role of bacterial multidrug efflux pumps in microbial natural ecosystems. *FEMS Microbiol Rev* 33:430–449. <https://doi.org/10.1111/j.1574-6976.2008.00157.x>.
13. Olivares Pacheco J, Alvarez-Ortega C, Alcalde Rico M, Martínez JL. 2017. Metabolic compensation of fitness costs is a general outcome for antibiotic-resistant *Pseudomonas aeruginosa* mutants overexpressing efflux pumps. *mBio* 8:e00500-17. <https://doi.org/10.1128/mBio.00500-17>.

14. Nishino K, Yamaguchi A. 2001. Overexpression of the response regulator *evgA* of the two-component signal transduction system modulates multidrug resistance conferred by multidrug resistance transporters. *J Bacteriol* 183:1455–1458. <https://doi.org/10.1128/JB.183.4.1455-1458.2001>.
15. Nishino K, Nikaido E, Yamaguchi A. 2007. Regulation of multidrug efflux systems involved in multidrug and metal resistance of *Salmonella enterica* serovar Typhimurium. *J Bacteriol* 189:9066–9075. <https://doi.org/10.1128/JB.01045-07>.
16. Marchand I, Damier-Piolle L, Courvalin P, Lambert T. 2004. Expression of the RND-type efflux pump AdeABC in *Acinetobacter baumannii* is regulated by the AdeRS two-component system. *Antimicrob Agents Chemother* 48:3298–3304. <https://doi.org/10.1128/AAC.48.9.3298-3304.2004>.
17. Perron K, Caille O, Rossier C, van Delden C, Dumas J-L, Köhler T. 2004. CzcR-CzcS, a two-component system involved in heavy metal and carbapenem resistance in *Pseudomonas aeruginosa*. *J Biol Chem* 279: 8761–8768. <https://doi.org/10.1074/jbc.M312080200>.
18. Fruci M, Poole K. 2018. Aminoglycoside-inducible expression of the *mexAB-oprM* multidrug efflux operon in *Pseudomonas aeruginosa*: Involvement of the envelope stress-responsive AmgRS two-component system. *PLoS One* 13:e0205036. <https://doi.org/10.1371/journal.pone.0205036>.
19. Muller C, Plésiat P, Jeannot K. 2011. A two-component regulatory system interconnects resistance to polymyxins, aminoglycosides, fluoroquinolones, and β -lactams in *Pseudomonas aeruginosa*. *Antimicrob Agents Chemother* 55:1211–1221. <https://doi.org/10.1128/AAC.01252-10>.
20. Scales BS, Erb-Downward JR, Huffnagle IM, LiPuma JJ, Huffnagle GB. 2015. Comparative genomics of *Pseudomonas fluorescens* subclade III strains from human lungs. *BMC Genomics* 16:1032. <https://doi.org/10.1186/s12864-015-2261-2>.
21. Liu X, Xiang L, Yin Y, Li H, Ma D, Qu Y. 2021. Pneumonia caused by *Pseudomonas fluorescens*: a case report. *BMC Pulm Med* 21:212. <https://doi.org/10.1186/s12890-021-01573-9>.
22. Pappas G, Karavasilis V, Christou L, Tsianos EV. 2006. *Pseudomonas fluorescens* infections in clinical practice. *Scand J Infect Dis* 38:68–70. <https://doi.org/10.1080/00365540500264043>.
23. Thangkhiew I. 1986. Successful treatment with ceftazidime of a *Pseudomonas fluorescens* chest infection in a myasthenic patient. *J Antimicrob Chemother* 18:428–429. <https://doi.org/10.1093/jac/18.3.428>.
24. Trivedi MKPS, Shettigar H, Gangwar M, Jana S. 2015. Antimicrobial sensitivity pattern of *Pseudomonas fluorescens* after biofield treatment. *Infectious Diseases and Therapy* 3:22. <https://doi.org/10.4172/2332-0877.1000222>.
25. Tian T, Wu X-G, Duan H-M, Zhang L-Q. 2010. The resistance-nodulation-division efflux pump EmhABC influences the production of 2,4-diacetylphloroglucinol in *Pseudomonas fluorescens* 2P24. *Microbiology (Reading)* 156:39–48. <https://doi.org/10.1099/mic.0.031161-0>.
26. Han J-T, Li D-Y, Zhang M-Y, Yu X-Q, Jia X-X, Xu H, Yan X, Jia W-J, Niu S, Kempfer ML, Tao X, He Y-X. 2021. EmhR is an indole-sensing transcriptional regulator responsible for the indole-induced antibiotic tolerance in *Pseudomonas fluorescens*. *Environ Microbiol* 23:2054–2069. <https://doi.org/10.1111/1462-2920.15354>.
27. Huang L, Xu W, Su Y, Zhao L, Yan Q. 2018. Regulatory role of the RstB-RstA system in adhesion, biofilm production, motility, and hemolysis. *Microbiologyopen* 7:e00599. <https://doi.org/10.1002/mbo3.599>.
28. Price MN, Wetmore KM, Waters RJ, Callaghan M, Ray J, Kuehl JV, Melnyk RA, Lamson JS, Suh Y, Esquivel Z, Sadeeshkumar H, Chakraborty R, Rubin BE, Bristow J, Blow MJ, Arkin AP, Deutschbauer AM. 2016. Deep annotation of protein function across diverse bacteria from mutant phenotypes. *bioRxiv* <https://doi.org/10.1101/072470.072470>.
29. Li Y-C, Chang C-k, Chang C-F, Cheng Y-H, Fang P-J, Yu T, Chen S-C, Li Y-C, Hsiao C-D, Huang T-H. 2014. Structural dynamics of the two-component response regulator RstA in recognition of promoter DNA element. *Nucleic Acids Res* 42:8777–8788. <https://doi.org/10.1093/nar/gku572>.
30. Affandi T, McEvoy MM. 2019. Mechanism of metal ion-induced activation of a two-component sensor kinase. *Biochem J* 476:115–135. <https://doi.org/10.1042/BCJ20180577>.
31. Whitchurch CB, Erova TE, Emery JA, Sargent JL, Harris JM, Semmler ABT, Young MD, Mattick JS, Wozniak DJ. 2002. Phosphorylation of the *Pseudomonas aeruginosa* response regulator AlgR is essential for Type IV fimbria-mediated twitching motility. *J Bacteriol* 184:4544–4554. <https://doi.org/10.1128/JB.184.16.4544-4554.2002>.
32. Tian Z-X, Yi X-X, Cho A, O'Gara F, Wang Y-P. 2016. CpxR activates *MexAB-OprM* efflux pump expression and enhances antibiotic resistance in both laboratory and clinical nalB-type isolates of *Pseudomonas aeruginosa*. *PLoS Pathog* 12:e1005932. <https://doi.org/10.1371/journal.ppat.1005932>.
33. Ringel MT, Brüser T. 2018. The biosynthesis of pyoverdines. *Microb Cell* 5: 424–437. <https://doi.org/10.15698/mic2018.10.649>.
34. Lamarche MG, Déziel E. 2011. MexEF-OprN efflux pump exports the *Pseudomonas* quinolone signal (PQS) precursor HHQ (4-hydroxy-2-heptylquinoline). *PLoS One* 6:e24310. <https://doi.org/10.1371/journal.pone.0024310>.
35. Piddock LJV. 2006. Clinically relevant chromosomally encoded multidrug resistance efflux pumps in bacteria. *Clin Microbiol Rev* 19:382–402. <https://doi.org/10.1128/CMR.19.2.382-402.2006>.
36. Horcajada JP, Montero M, Oliver A, Sorlí L, Luque S, Gómez-Zorrilla S, Benito N, Grau S. 2019. Epidemiology and treatment of multidrug-resistant and extensively drug-resistant *Pseudomonas aeruginosa* infections. *Clin Microbiol Rev* 32:e00031-19. <https://doi.org/10.1128/CMR.00031-19>.
37. Trastoy R, Manso T, Fernández-García L, Blasco L, Ambroa A, Pérez Del Molino ML, Bou G, García-Contreras R, Wood TK, Tomás M. 2018. Mechanisms of bacterial tolerance and persistence in the gastrointestinal and respiratory environments. *Clin Microbiol Rev* 31. <https://doi.org/10.1128/CMR.00023-18>.
38. Jeon J, Kim H, Yun J, Ryu S, Groisman EA, Shin D. 2008. RstA-promoted expression of the ferrous iron transporter FeoB under iron-replete conditions enhances fur activity in *Salmonella enterica*. *J Bacteriol* 190: 7326–7334. <https://doi.org/10.1128/JB.00903-08>.
39. Ogasawara H, Hasegawa A, Kanda E, Miki T, Yamamoto K, Ishihama A. 2007. Genomic SELEX search for target promoters under the control of the PhoQP-RstBA signal relay cascade. *J Bacteriol* 189:4791–4799. <https://doi.org/10.1128/JB.00319-07>.
40. Robinson VL, Wu T, Stock AM. 2003. Structural analysis of the domain interface in DrrB, a response regulator of the OmpR/PhoB subfamily. *J Bacteriol* 185:4186–4194. <https://doi.org/10.1128/JB.185.14.4186-4194.2003>.
41. Fol M, Chauhan A, Nair NK, Maloney E, Moomey M, Jagannath C, Madiraju MVVS, Rajagopalan M. 2006. Modulation of mycobacterium tuberculosis proliferation by MtrA, an essential two-component response regulator. *Mol Microbiol* 60:643–657. <https://doi.org/10.1111/j.1365-2958.2006.05137.x>.
42. Gushchin I, Melnikov I, Polovinkin V, Ishchenko A, Yuzhakova A, Buslaeva P, Bourenkov G, Grudinin S, Round E, Balandin T, Borschchevskiy V, Willbold D, Leonard G, Büldt G, Popov A, Gordeliy V. 2017. Mechanism of transmembrane signaling by sensor histidine kinases. *Science* 356:eaah6345. <https://doi.org/10.1126/science.aah6345>.
43. Stewart V. 1993. Nitrate regulation of anaerobic respiratory gene expression in *Escherichia coli*. *Mol Microbiol* 9:425–434. <https://doi.org/10.1111/j.1365-2958.1993.tb01704.x>.
44. Noriega CE, Lin H-Y, Chen L-L, Williams SB, Stewart V. 2010. Asymmetric cross-regulation between the nitrate-responsive NarX–NarL and NarQ–NarP two-component regulatory systems from *Escherichia coli* K-12. *Mol Microbiol* 75:394–412. <https://doi.org/10.1111/j.1365-2958.2009.06987.x>.
45. Philippot L, Mirleau P, Mazurier S, Siblot S, Hartmann A, Lemanceau P, Germon JC. 2001. Characterization and transcriptional analysis of *Pseudomonas fluorescens* denitrifying clusters containing the *nar*, *nir*, *nor* and *nos* genes. *Biochimica et Biophysica Acta (BBA) - Gene Structure and Expression* 1517:436–440. [https://doi.org/10.1016/S0167-4781\(00\)00286-4](https://doi.org/10.1016/S0167-4781(00)00286-4).
46. Noriega CE, Schmidt R, Gray MJ, Chen L-L, Stewart V. 2008. Autophosphorylation and dephosphorylation by soluble forms of the nitrate-responsive sensors NarX and NarQ from *Escherichia coli* K-12. *J Bacteriol* 190: 3869–3876. <https://doi.org/10.1128/JB.00092-08>.
47. Maghnoji A, de Sousa Cabral TF, Stalon V, Vander Wauven C. 1998. The arcABDC gene cluster, encoding the arginine deiminase pathway of *Bacillus licheniformis*, and its activation by the arginine repressor argR. *J Bacteriol* 180:6468–6475. <https://doi.org/10.1128/JB.180.24.6468-6475.1998>.
48. Muriel C, Jalvo B, Redondo-Nieto M, Rivilla R, Martín M. 2015. Chemotactic motility of *Pseudomonas fluorescens* F113 under aerobic and denitrification conditions. *PLoS One* 10:e0132242. <https://doi.org/10.1371/journal.pone.0132242>.
49. Hausladen A, Gow AJ, Stamler JS. 1998. Nitrosative stress: metabolic pathway involving the flavohemoglobin. *Proc Natl Acad Sci USA* 95: 14100–14105. <https://doi.org/10.1073/pnas.95.24.14100>.
50. Zhang Y, Xiao M, Horiyama T, Zhang Y, Li X, Nishino K, Yan A. 2011. The multidrug efflux pump MdtEF protects against nitrosative damage during the anaerobic respiration in *Escherichia coli*. *J Biol Chem* 286:26576–26584. <https://doi.org/10.1074/jbc.M111.243261>.
51. Fetar H, Gilmour C, Klinoski R, Daigle DM, Dean CR, Poole K. 2011. *mexEF-oprN* multidrug efflux operon of *Pseudomonas aeruginosa*: regulation by the MexT activator in response to nitrosative stress and chloramphenicol. *Antimicrob Agents Chemother* 55:508–514. <https://doi.org/10.1128/AAC.00830-10>.

52. Firoved AM, Wood SR, Ornatowski W, Deretic V, Timmins GS. 2004. Microarray analysis and functional characterization of the nitrosative stress response in nonmucoid and mucoid *Pseudomonas aeruginosa*. *J Bacteriol* 186:4046–4050. <https://doi.org/10.1128/JB.186.12.4046-4050.2004>.
53. Schwalbe R, Steele-Moore L, Goodwin AC. 2007. Antimicrobial susceptibility testing protocols. CRC Press, Boca Raton, FL.
54. Yan X, Yang R, Zhao R-X, Han J-T, Jia W-J, Li D-Y, Wang Y, Zhang N, Wu Y, Zhang L-Q, He Y-X. 2017. Transcriptional regulator PhIH modulates 2,4-diacetylphloroglucinol biosynthesis in response to the biosynthetic intermediate and end product. *Appl Environ Microbiol* 83:e01419–17. <https://doi.org/10.1128/AEM.01419-17>.
55. Miller JH. 1972. Experiments in molecular genetics. Cold Spring Harbor Laboratory Press, Cold Spring Harbor, NY.
56. Pogliano J, Lynch AS, Belin D, Lin EC, Beckwith J. 1997. Regulation of *Escherichia coli* cell envelope proteins involved in protein folding and degradation by the Cpx two-component system. *Genes Dev* 11:1169–1182. <https://doi.org/10.1101/gad.11.9.1169>.
57. Kulak NA, Pichler G, Paron I, Nagaraj N, Mann M. 2014. Minimal, encapsulated proteomic-sample processing applied to copy-number estimation in eukaryotic cells. *Nat Methods* 11:319–324. <https://doi.org/10.1038/nmeth.2834>.
58. Carvalho PC, Fischer JSG, Chen EI, Yates JR, Barbosa VC. 2008. PatternLab for proteomics: a tool for differential shotgun proteomics. *BMC Bioinformatics* 9:316. <https://doi.org/10.1186/1471-2105-9-316>.
59. Cox J, Mann M. 2012. 1D and 2D annotation enrichment: a statistical method integrating quantitative proteomics with complementary high-throughput data. *BMC Bioinformatics* 13 Suppl 16:S12. <https://doi.org/10.1186/1471-2105-13-S16-S12>.
60. Vizcaino JA, Csordas A, del-Toro N, Dienes JA, Griss J, Lavidas I, Mayer G, Perez-Riverol Y, Reisinger F, Ternent T, Xu QW, Wang R, Hermjakob H. 2016. 2016 update of the PRIDE database and its related tools. *Nucleic Acids Res* 44:D447–56. <https://doi.org/10.1093/nar/gkv1145>.